THE JOURNAL OF PHYSICAL CHEMISTRY A LETTERS

2007, *111,* 8286−8290
Published on Web 08/08/2007

Significant Nonadiabatic Effects in the S(^{1}D) + HD Reaction

Tian-Shu Chu,[†] Ke-Li Han,*[,†] and George C. Schatz[‡]

State Key Laboratory of Molecular Reaction Dynamics, Dalian Institute of Chemical Physics, Chinese Academy of Science, Dalian 116023, China, and Department of Chemistry, Northwestern University, Evanston, Illinois 60208-3113

Received: July 3, 2007

A nonadiabatic quantum dynamics calculation involving four coupled potential energy surfaces (two degenerate ^{3}A″, one ^{3}A′, and one ^{1}A′) and the spin−orbit coupling matrix for these states is reported for the title reaction. The results show that the important discrepancy between theoretically calculated and experimentally measured intramolecular isotope effects can at least in part be attributed to significant nonadiabatic effects.

The S(^{1}D) + H_2 reaction and its isotopic variants, together with O(^{1}D) + H_2, N(^{2}D) + H_2, C(^{1}D) + H_2, etc., are paradigms for reactions that involve insertion dynamics.[1−3] A number of detailed quasi-classical trajectory and quantum mechanical (QM) reactive-scattering calculations have been reported for S(^{1}D) + H_2 on the lowest singlet state (^{1}A′) potential energy surface.[4−13] Recent molecular beam experiments have also probed the dynamics of this system at low-collision energies.[14−16] While there is satisfactory agreement between most experimental and calculated results, a very significant discrepancy still exists between experiment[16] and earlier QM calculations[12,13] for the S(^{1}D) + HD intramolecular isotope effect, defined as $r' = \sigma_{SH+D}/\sigma_{SD+H}$ with σ being the reactive integral cross section. The striking observation of the experimental results is that r' has a nonstatistical value of roughly 1.3∼1.4 for collision energies below 0.3 eV.[16] Past theoretical calculations have estimated this ratio to be ∼1, which is what would be expected from statistical theory.[12,13] The discrepancy between theory and experiment has been attributed to the detection method,[10,12] to the dynamics treatment, to nonadiabatic effects,[13] etc. Among these, we believe that nonadiabatic effects are the most likely. As will be described below, intersystem crossing can play an important role for this isotopic variant, possibly large enough to account for the observed nonstatistical feature in the intramolecular isotope effect. Therefore, performing nonadiabatic investigations of the title reaction might help to unravel the apparent paradox between theory and experiment.

Similar to O(^{1}D,^{3}P) + H_2,[17,18] intersystem crossing can occur in the S(^{1}D,^{3}P) + H_2 reactive system due to spin−orbit coupling of the singlet/triplet states. In particular, intersystem crossing can play an important role if the spin-forbidden state drops below the initial spin state to provide a new pathway for reaction to occur and if nonadiabatic dynamics is sufficiently important. Recent studies of intersystem-crossing effects revealed modest/subtle nonadiabatic effects for the O(^{1}D,^{3}P) + H_2 reaction,[17−21] which is understandable because the locations of the crossing seam along the minimum energy path of the triplet reaction are on the product side of the triplet barrier in this system.[18] For S + H_2, however, the crossing is located before the triplet barrier on the reactant side and below the asymptotic energy of the product.[22] This difference in crossing locations in conjunction with a factor of 3 larger spin−orbit coupling in the heavier S + H_2 system[22] suggests that nonadiabatic effects can be more pronounced than with O + H_2. The prediction was verified in a recent trajectory surface-hopping (TSH) study of intersystem-crossing effects in S + H_2 by Maiti et al.[22] with the significant role of intersystem crossing being revealed in the reaction dynamics especially at low-collision energy. Except for this study, no other theoretical dynamics investigations aimed at clarifying this prediction have been reported for the S + H_2 or its isotopic variants so far.

The title reaction presents what is likely the most difficult dynamical system ever studied for QM studies, not only because there is a deep potential well on the ground singlet surface,[7] but also because there is no permutational symmetry of the three atoms involved and because there are four interacting electronic potential surfaces in the multisurface dynamics. This explains why no quantum-scattering studies of nonadiabatic effects have been published thus far for the title reaction.

In this work, we present a quantum nonadiabatic study of S(^{1}D) + HD using the time-dependent wave packet approach with a split-operator scheme.[23,24] Using this methodology, we computed integral cross sections for both the adiabatic channel and the spin-forbidden nonadiabatic channels of the S(^{1}D) + HD ($v = j = 0$) reaction. We further calculated the intramolecular isotope effect and compared it with the experimental data. Significant nonadiabatic effects have been found for this isotopic variant, and the calculated isotope effect with nonadiabatic effects included is noticeably closer to the experimental measurements, thus suggesting that nonadiabatic effects play a role in unraveling the discrepancy between theory and experiment.

Four potential energy surfaces, two degenerate ^{3}A″ states, one ^{3}A′,[22] and one ^{1}A′ state,[7] were used in the present quantum calculations, along with the spin−orbit coupling matrix among these states.[22] These four states constitute the subset of states

* To whom correspondence should be addressed. Email: klhan@dicp.ac.cn.
† Chinese Academy of Science.
‡ Northwestern University.

10.1021/jp075173q CCC: $37.00

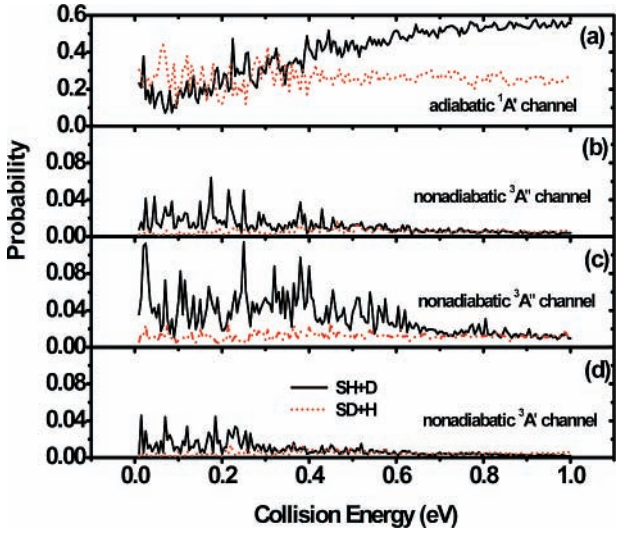

Figure 1. Calculated reaction probabilities for $J = 0$ as a function of collision energy over the range of 0.01−1.0 eV for the S(^{1}D) + HD ($v = 0$, $j = 0$) reaction. Here, the wave packet is initially in the singlet ^{1}A′ state. (a) adiabatic ^{1}A′ channel. (b−d) nonadiabatic ^{3}A″(first), ^{3}A″(second), and ^{3}A′ channels. Solid line refers to the SH + D product, short-dashed line refers to the SD + H product.

correlating to S(^{3}P, ^{1}D) + H_2 that are coupled to the initially populated ^{1}A′ state. Although five states asymptotically correlate to S(^{1}D), only the lowest ^{1}A′ state leads to insertion, so it likely dominates the initial stages of the reaction dynamics. Also, this state is the only one that crosses the triplet states at low energies, and therefore it is the most likely singlet state to be involved in intersystem crossing.

Details of the decoupling of the multistate reaction dynamics into dynamics involving these four states was developed for the O(^{3}P) + H_2 reaction by Hoffmann and Schatz,[17] and the same approach applies analogously to S(^{3}P, ^{1}D) + H_2. In the present quantum calculation with the wave packet initially in the ^{1}A′ state, 420 translational basis functions in the R range 0.1−16.0 a_0, 210 vibrational basis functions in the r range 0.5−15.0 a_0, and $j_{max} = 100$ rotational basis functions are used to converge the calculated results after a propagation time of 100 000 au. The position to perform the flux analysis is chosen at $r = 11.0$ a_0. Further, two strategies are implemented to overcome the computational challenges associated with this system. First, we used OpenMP parallel quantum dynamics during the calculation. Second, we computed the reaction probabilities only for $J = 0$−20, 25, 30, 35....60; for other J, we employed a capture model calculation proposed by Gray et al.[25,26] The computation time for each J is about 4833 h using Max 2-way AMD Opteron 200 series dual-core processors from Dawning R210A, demonstrating that the present calculation is very challenging.

Figure 1 shows the calculated $J = 0$ reaction probabilities as a function of collision energy in the range 0.01−1.0 eV for the adiabatic and nonadiabatic formation of the SH + D and SD + H products in the S(^{1}D) + HD ($v = 0$, $j = 0$) reaction. Here, the initial wave packet starts in ^{1}A′, and the adiabatic channel refers to ^{1}A′→^{1}A′, while the nonadiabatic channels are ^{1}A′→^{3}A″, ^{3}A′. Note that all results are generated from the multistate calculations, so the adiabatic channel still includes contributions from nonadiabatic dynamics. For the adiabatic ^{1}A′ channel, we see that at very low-collision energies, SD + H shows slightly larger reaction probabilities than SH + D, while the branching is reversed at high-collision energies. There is an overall increasing/decreasing trend with increasing collision energy in

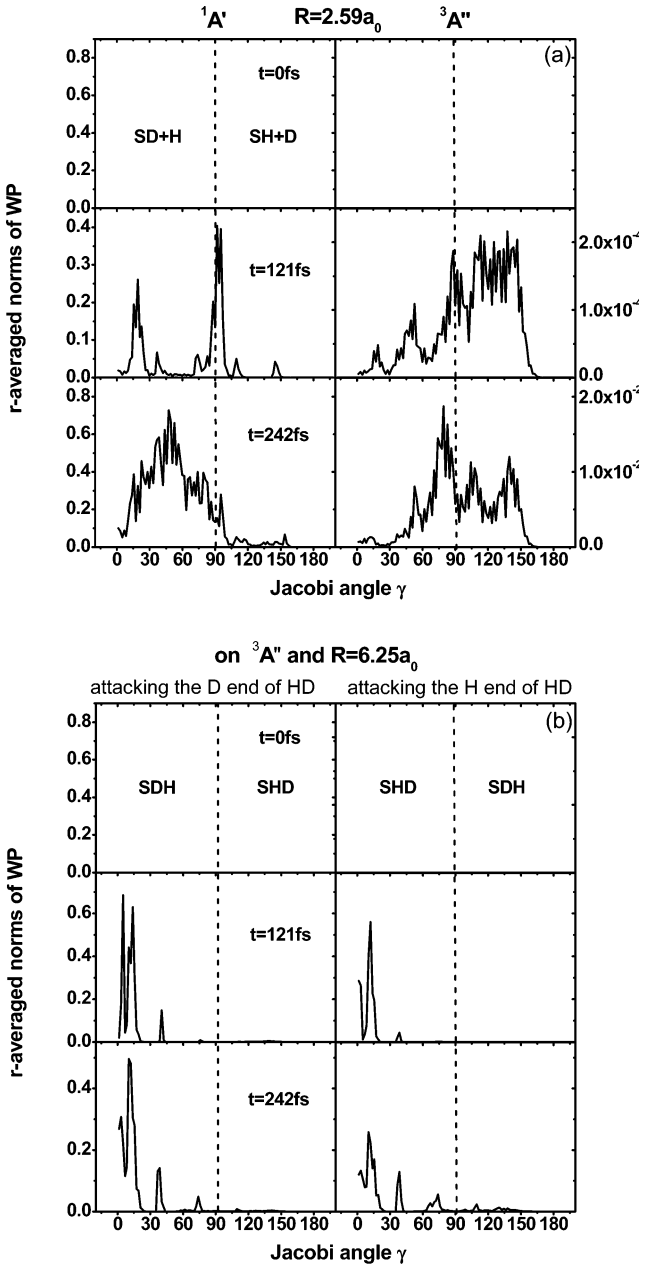

Figure 2. The r-averaged norms of WP at three times using reactant Jacobi coordinates (R, r, γ). (a) On both ^{1}A′ and ^{3}A″ near the transition state on the product side ($R = 2.59$ a_0) when the S atom collinearly attacks the D end of HD. (b) On ^{3}A″ at the reactant side ($R = 6.25$ a_0) when the S atom collinearly attacks the D end and the H end of HD, respectively.

the whole energy range for the SH + D and SD + H products, respectively. The same $J = 0$ adiabatic behavior has also been revealed for this isotopic variant in single-surface calculations.[12,13] When we examine the results obtained on the three triplet surfaces (two ^{3}A″ and one ^{3}A′), we find that for the nonadiabatic ^{3}A″/^{3}A′ channels the reaction probabilities for SH + D are always larger than those for SD + H, particularly for low-collision energies (E_c < 0.3 eV).

There are several reasons why the nonadiabatic formation of the SH + D product is favored over that for SD + H. The intensity of nonadiabatic transitions is likely higher for SH + D, as this involves more motion of the lighter, more rapidly moving H atom. Tunneling effects and zero-point energy differences are probably also important, because the nonadiabatic formation of products requires the reactant to surmount the

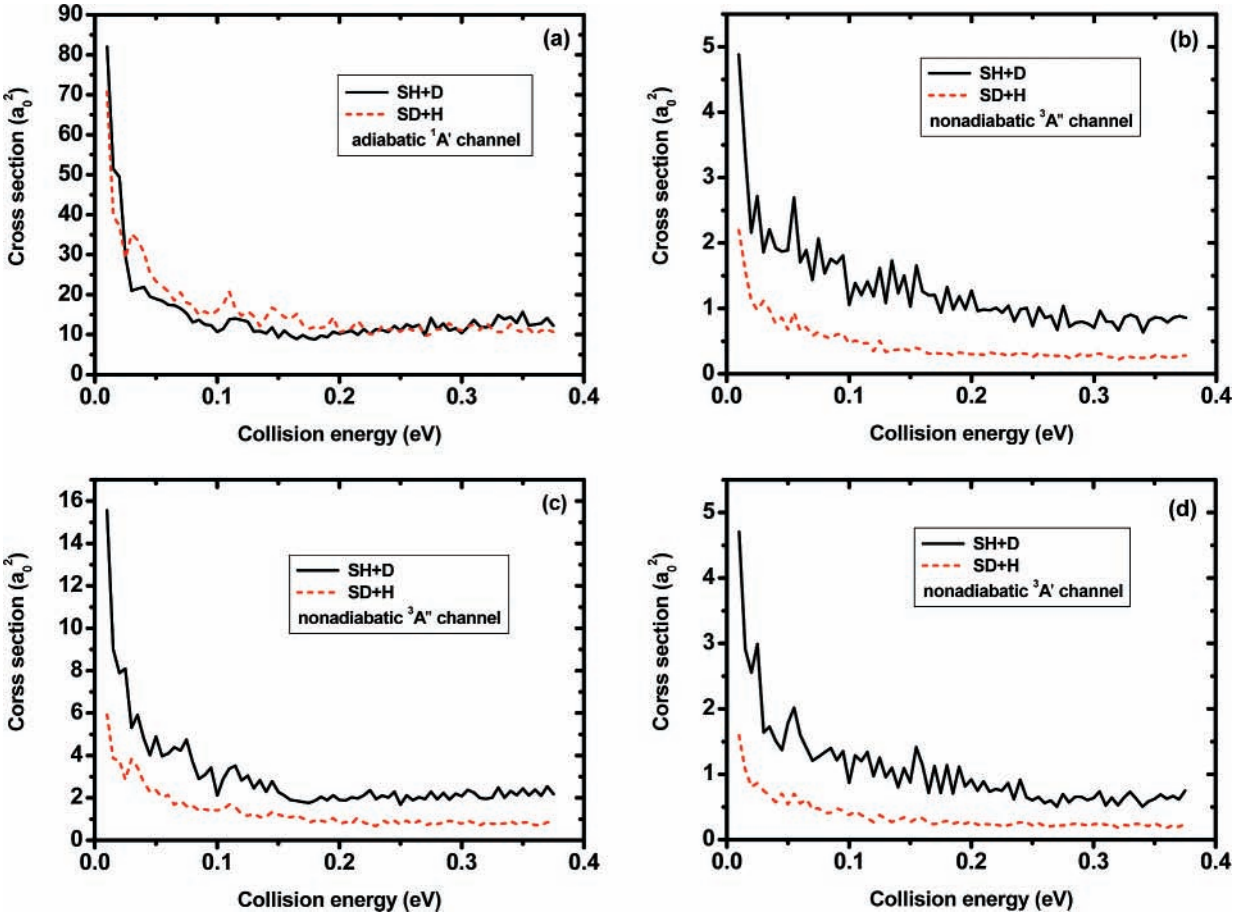

Figure 3. Similar to Figure 1, but for the integral cross sections in the collision energy range of 0.01−0.4 eV. (a) Adiabatic 1A channel, (b−d) nonadiabatic 3A (first), 3A (second), and 3A channels.

triplet barriers. To help clarify this, in Figure 2, we plot snapshots of the wave packet (WP), that is, *r*-averaged norms versus angle γ using reactant Jacobi coordinates (R, r, γ) at three times. Figure 2a shows the WP on both ^{1}A′ and ^{3}A″ near the transition state on the product side ($R = 2.59$ a_0) for initial conditions where the S atom collinearly attacks the D end of the HD molecule. Figure 2b shows the WP just on ^{3}A″ for a value of R that corresponds to the reactant side ($R = 6.25$ a_0) for two sets of initial conditions: (1) the S atom collinearly attacks the D end of HD (left panel), and (2) the S atom collinearly attacks the H end of HD (right panel). It can be seen that the nonadiabatic channel shows a different angle-dependent behavior from the adiabatic channel near the transition state (see Figure 2a) with more reactive flux going to SH + D. Further, quenching to S(^{3}P) + HD is much higher for angles corresponding to SDH than SHD (that is, the SDH flux in Figure 2b is higher than SHD). It is therefore apparent that quenching kills the flux that would have gone to produce SD + H and leads to the overall preference of SH + D over SD + H formed via the nonadiabatic channels. The reason for this presumably lies in the slow motion of the D atom as this makes quenching more efficient than reaction after flux is transferred to the ^{3}A″ state. Of the three nonadiabatic channels, the one associated with the second ^{3}A″ surface (as shown in Figure 1c) has the largest reaction probabilities, thus indicating that the nonadiabatic dynamics on this surface is the most significant one. This result is consistent with the earlier TSH study of S(^{3}P) + H_2 in which more significant intersystem-crossing dynamics to the ^{1}A′ state was found when trajectories started on the ^{3}A″ surface.[22] The other two nonadiabatic channels are found to have similar but smaller nonadiabatic effects.

Figure 3 shows the calculated integral cross sections for the S + HD ($v = 0$, $j = 0$) reaction over the collision energy range of 0.01−0.4 eV. For the adiabatic ^{1}A′ channel, as shown in Figure 3a, the SD + H product is slightly favored over SH + D for collision energies between 0.03 and 0.2 eV; outside this range they become very close to each other. In contrast to this, a strong preference was found for the SH + D product formed via intersystem crossing due to the different reaction dynamics on the triplet surfaces. As in Figure 1, the second ^{3}A″ dynamics is the dominant contributor to the nonadiabatic formation of the products, while the ^{3}A′ dynamics has almost the same contribution as the first ^{3}A″ dynamics with a slight preference being found for the first ^{3}A″ dynamics. The nonadiabatic transition cross section contributes 20∼35% and 9∼14% to the total cross sections for the SH + D and SD + H products, respectively. Compared with our previously calculated 1.6∼2.2% contributions from the nonadiabatic cross sections for O(^{1}D) + H_2,[21] the results clearly show that there are more significant nonadiabatic effects for the S + HD reaction.

Figure 4 compares the present nonadiabatic quantum calculation with the recent single surface quantum real wave packet dynamics study using a *J*-shifting method.[27] The figure shows that the sum of the present reactive cross sections over the four electronic states is lower than the single-surface quantum result[27] for the SH + D and SD + H products. This is probably due to the significant electronic quenching of S(^{1}D) + HD to S(^{3}P) + HD because the singlet−triplet crossing of the reaction system is located before the triplet barrier. To clarify this, we present in Figure 5 the calculated quenching cross sections, along with the total reactive cross sections that sum over the SH + D and SD + H products (both the adiabatic and nonadiabatic channels

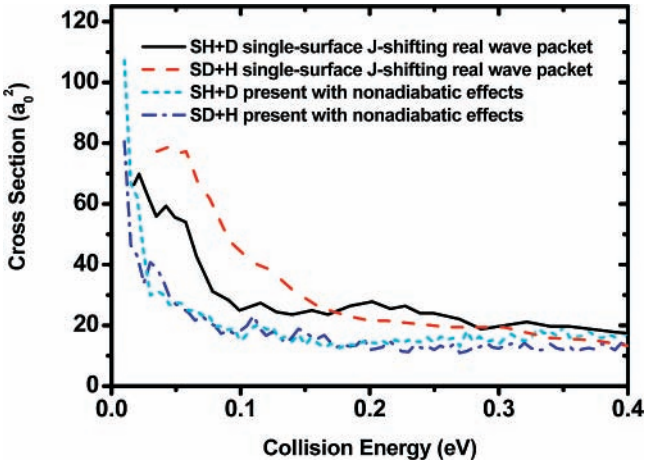

Figure 4. A comparison between the present calculation and the single-surface quantum dynamics study using a *J*-shifting method (ref 27). Solid and dashed lines refer to the adiabatic *J*-shifting cross sections for SH + D and SD + H, respectively. Short-dashed and dash-dotted lines show the present cross sections that have been summed over the adiabatic and nonadiabatic channels for SH + D and SD + H, respectively.

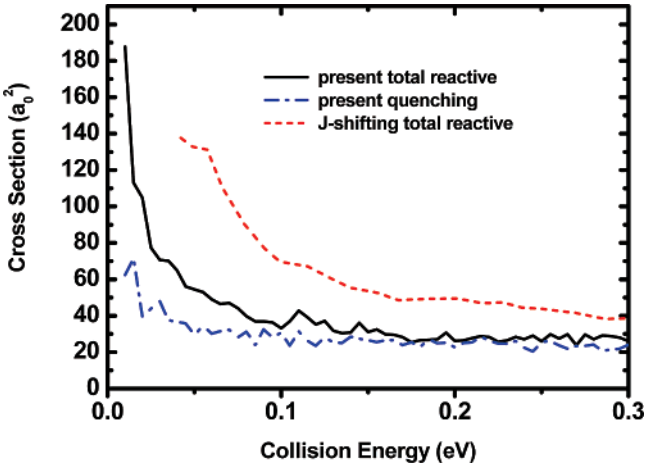

Figure 5. Electronic-quenching cross section (dash-dotted line) leading to $S(^3P)$ + HD as a function of collision energy, along with the total reactive cross sections summing over the SH + D and SD + H products (present including the adiabatic and nonadiabatic channels in solid line and the single-surface calculation from ref 27 in the short-dashed line).

are included). The single-surface quantum results[27] are also presented for comparison. These results show that there exists strong electronic quenching comparable to the reactive cross section, which is responsible for the difference between the present and the single-surface reactive cross sections.[27] Note that significant quenching was also revealed in the TSH study of S + H_2 in ref 22. Thus the results confirm the significance of the nonadiabatic effects/intersystem crossing for the title reaction.

Figure 6 presents the branching ratio $\sigma_{SH+D}/\sigma_{SD+H}$ corresponding to the adiabatic and nonadiabatic channels, respectively. Clearly, the adiabatic channel shows statistical behavior with a value around close to unity based on an insertion reaction mechanism. This is consistent with earlier single-surface results from a *J*-shifting/capture model.[13] But the intramolecular-branching ratio has a high value for the nonadiabatic channels (averaging about 2.5) that is far from statistical. As can be seen, the experimental results[16] are higher than the adiabatic-branching ratios but lower than the nonadiabatic ones; this therefore raises

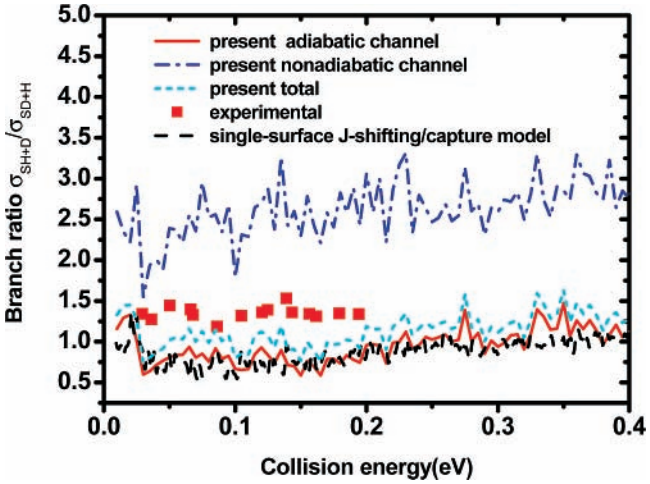

Figure 6. Intramolecular isotope effect (branching ratio $\sigma_{SH+D}/\sigma_{SD+H}$) for the adiabatic (solid line) and the nonadiabatic (dash-dotted line), all including the adiabatic and nonadiabatic (short-dashed line) channels, respectively. The experimental results (solid square, ref 16) and the single-surface *J*-shifting/capture model wave packet results (dashed line, ref 13) are also shown for comparison.

the interesting question of "to which extent will nonadiabaticity influence the overall branching ratio for this isotopic variant"? With this in mind, we have calculated the intramolecular isotope effect including both adiabatic and nonadiabatic channels, and the corresponding results are included in Figure 6. As can be seen, due to the contribution of the nonadiabatic transitions the branching ratio has a value of 1.3 at low energies, dropping to 1.1 at higher energies. These results are closer to the experimental result of Liu and co-workers[16] than is obtained from single-surface calculations. Thus, this calculation confirms that nonadiabatic effects are very important for the title reaction, and that this nonadiabaticity influences the intramolecular isotope effect, resulting in a moderate shift from the statistical value.

Acknowledgment. This work is supported by NSFC (20333050, 20573110, and 20633070). G.C.S. was supported by AFOSR Grant FA9550-07-1-0095.

References and Notes

(1) Casavecchia, P. *Rep. Prog. Phys.* **2000**, *63*, 355.
(2) Liu, K. *Annu. Rev. Phys. Chem.* **2001**, *52*, 139.
(3) Althorpe, S. C.; Clary, D. C. *Annu. Rev. Phys. Chem.* **2003**, *54*, 493.
(4) Chang, H. H.; Lin, S. H. *Chem. Phys. Lett.* **2000**, *320*, 161.
(5) Zyubin, S.; Mebel, A. M.; Chao, S. D.; Skodje, R. T. *J. Chem. Phys.* **2001**, *114*, 320.
(6) Chao, S. D.; Skodje, R. T. *J. Phys. Chem.* **2001**, *105*, 2474.
(7) Ho, T.-S.; Hollebeek, T.; Rabitz, H.; Chao, S. D.; Skodje, R. T.; Zyubin, A. S.; Mebel, A. M. *J. Chem. Phys.* **2002**, *116*, 4124.
(8) Honvault, P.; Launay, J.-M. *Chem. Phys. Lett.* **2003**, *370*, 371.
(9) Rackham, E. J.; Gonzalez-Lezana, T.; Manolopoulos, D. E. *J. Chem. Phys.* **2003**, *119*, 12895.
(10) Bañares, L.; Aoiz, F. J.; Honvault, P.; Launay, J.-M. *J. Phys. Chem. A* **2004**, *108*, 1616.
(11) Mouret, L.; Launay, J.-M.; Terao-Dunseath, M.; Dunseath, K. *Phys. Chem. Chem. Phys.* **2004**, *6*, 4105.
(12) Bañares, L.; Castillo, J. F.; Honvault, P.; Launay, J.-M. *Phys. Chem. Chem. Phys.* **2005**, *7*, 627.
(13) Lin, S. Y.; Guo, H. *J. Chem. Phys.* **2005**, *122*, 074304.
(14) Lee, S.-H.; Liu, K. *Appl. Phys. B* **2000**, *71*, 627.
(15) Lee, S.-H.; Liu, K. *J. Phys. Chem. A* **1998**, *102*, 8637.
(16) Lee, S.-H.; Liu, K. *Chem. Phys. Lett.* **1998**, *290*, 323.
(17) Hoffmann, M. R.; Schatz, G. C. *J. Chem. Phys.* **2000**, *113*, 9456.
(18) Maiti, B.; Schatz, G. C. *J. Chem. Phys.* **2003**, *119*, 12360.

(19) Braunstein, M.; Adler-Golden, S.; Maiti, B.; Schatz, G. C. *J. Chem. Phys.* **2004**, *120*, 4316.

(20) Balakrishnan, N. *J. Chem. Phys.* **2004**, *121*, 6346.

(21) Chu, T. S.; Zhang, X.; Han, K. L. *J. Chem. Phys.* **2005**, *122*, 214301.

(22) Maiti, B.; Schatz, G. C.; Lendvay, G. *J. Phys. Chem. A* **2004**, *108*, 8772.

(23) Xie, T. X.; Zhang, Y.; Zhao, M. Y.; Han, K. L. *Phys. Chem. Chem. Phys.* **2003**, *5*, 2034.

(24) Chu, T. S.; Zhang, Y.; Han, K. L. *Int. Rev. Phys. Chem.* **2006**, *25*, 201.

(25) Gray, S. K.; Goldfield, E. M.; Schatz, G. C.; Balint-Kurti, G. G. *Phys. Chem. Chem. Phys.* **1999**, *1*, 1141.

(26) Gray, S. K.; Balint-Kurti, G. G.; Schatz, G. C.; Lin, J. J.; Liu, X.; Harich, S.; Yang, X. *J. Chem. Phys.* **2000**, *113*, 7330.

(27) Gogtas, F.; Bulut, N.; Akpinar, S. *J. Mol. Struct.* (*THEOCHEM*) **2005**, *723*, 189.